Electronic Supplementary Material (ESI) for Physical Chemistry Chemical Physics.

Exploiting the photophysical features of DMAN template in ITQ-51 zeotype in the search for FRET energy transfer

SUPPORTING INFORMATION

Ainhoa Oliden-Sánchez[a], Rebeca Sola-Llano[a], Joaquín Pérez-Pariente[b], Luis Gómez-Hortigüela[b]* and Virginia Martínez-Martínez[a]*

[a]Departamento de Química Física, Universidad del País Vasco (UPV/EHU), Apartado 644, 4808 Bilbao, Spain; ainhoa.oliden@ehu.eus, rebeca.sola@ehu.eus, virginia.martinez@ehu.eus

[b]Instituto de Catálisis y Petroleoquímica. CSIC, c/ Marie Curie 2, 28049 Cantoblanco, Madrid, Spain; lhortiguela@icp.csic.es, jperez@icp.csic.es

*Correspondence: lhortiguela@icp.csic.es and virginia.martinez@ehu.eus

1. Synthesis procedure, gel composition and XRD profiles of Mg-ITQ-51 samples

Table S1. Specific gel molar compositions for the as-synthesized Dye/Mg-ITQ-51 hybrid systems.

Sample	Al_2O_3	P_2O_5	MgO	DMAN	H_2O	Dye
MgIFO-1	0.95	1.00	0.10	1.21	39.92	-
R123/MgIFO-1	0.95	1.00	0.10	1.20	40.19	0.008 R123
NB/MgIFO-1	0.94	0.99	0.10	1.22	42.59	0.008 NB

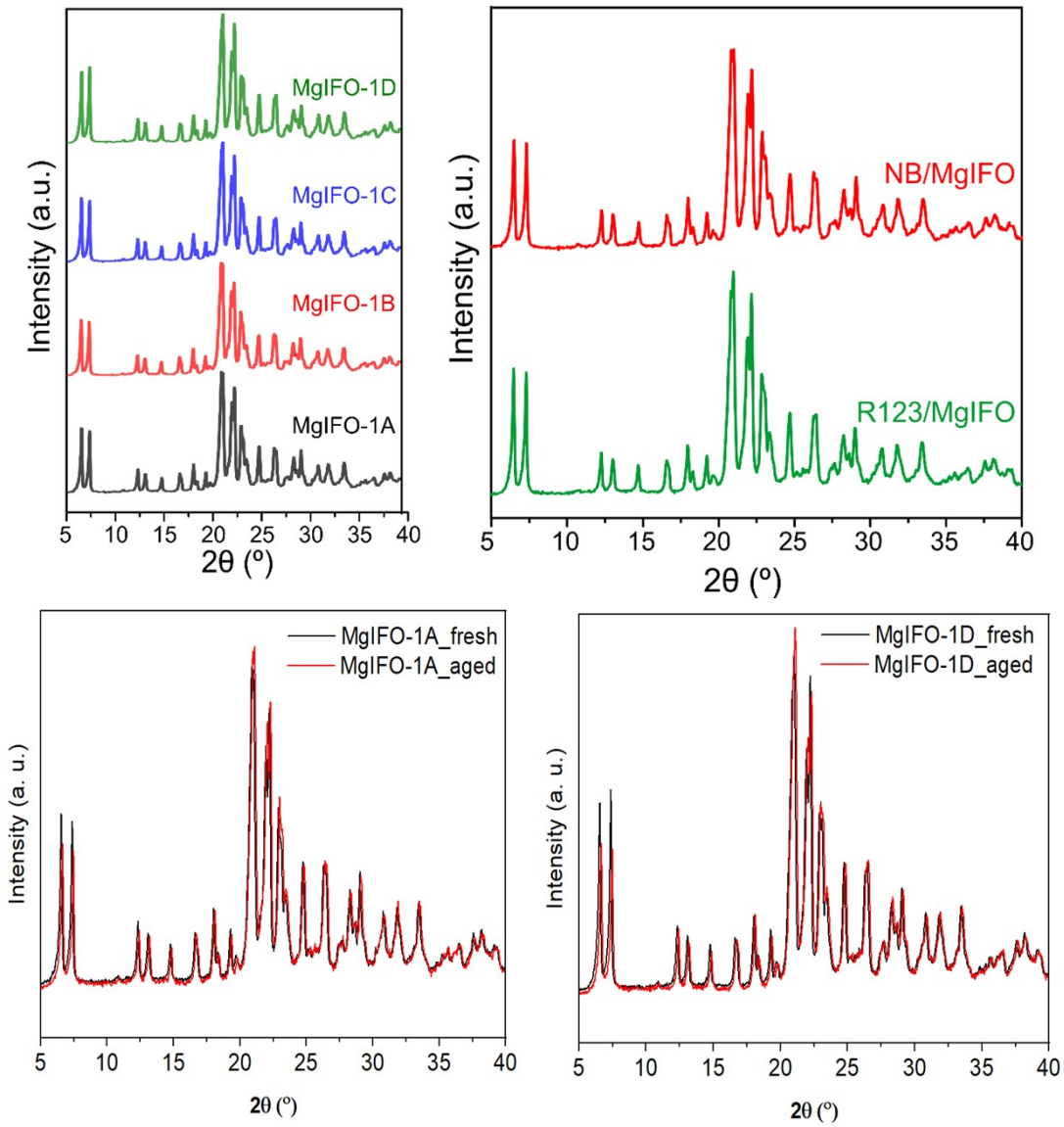

Figure S1. Top: PXRD patterns for (left) MgIFO-1 samples at different heating times. A = 1, B = 2, C = 3 and D = 5 days and dye-doped MgIFO samples (right). Bottom: XRD patterns of samples A (left) and D (right) fresh (black) and after long-term aging (red).

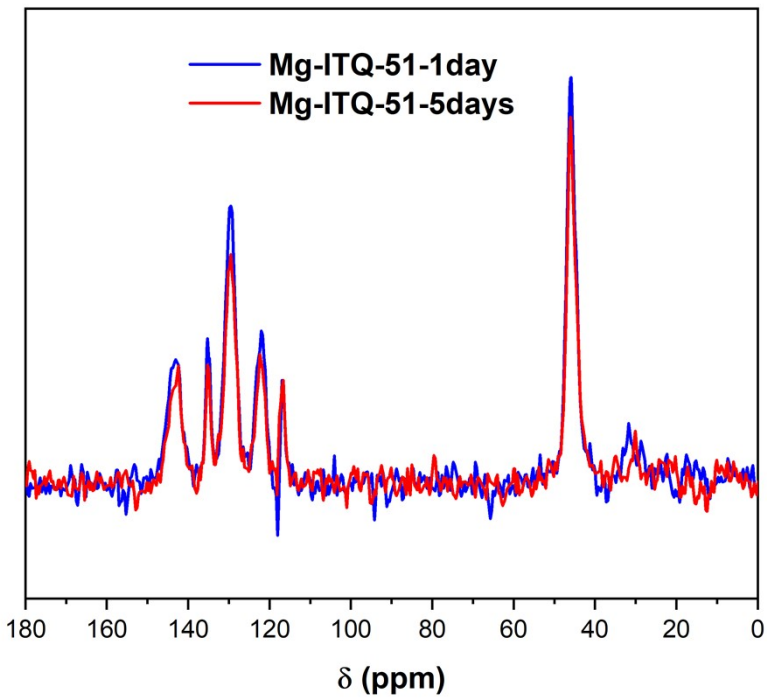

Figure S2. ^{13}C CP MAS NMR of Mg-ITQ-51 samples obtained after 1 (blue) and 5 (red) days of crystallization.

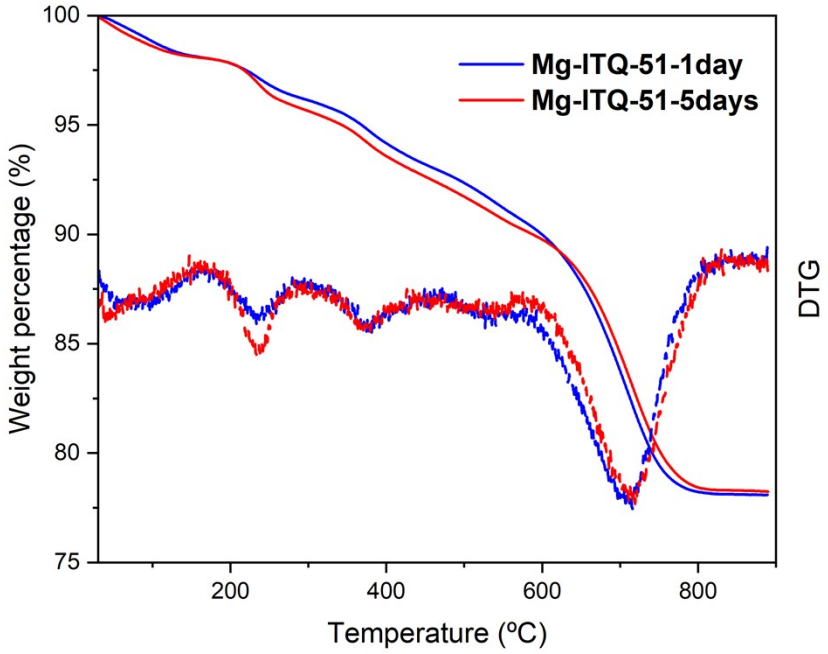

Figure S3. TGA of Mg-ITQ-51 samples obtained after 1 (blue) or 5 (red) days of crystallization.

Table S2. CHN elemental analysis of Mg-ITQ-51 samples obtained after 1 or 5 days of crystallization.

Sample	% C	% H	% N	C/N	% DMAN
Mg-ITQ-51-1day	13.47	2.10	2.39	6.6 (7)	17.24
Mg-ITQ-51-5day	13.93	2.00	2.39	6.8 (7)	17.83

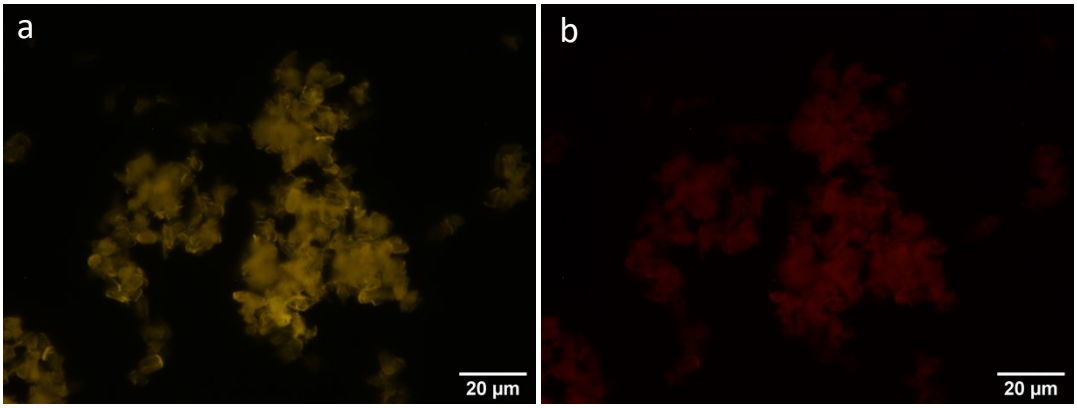

Figure S4. Fluorescence images of MgIFO sample (1 day after the synthesis) using (a) D470/70 excitation band pass filter, 495DCLP dichroic and E515LPv2 cut-off; (b) HQ530/30m excitation band pass filter, Q660LP dichroic and E580lp cut-off.

2. Photophysics of DMAN in solution

The photophysics of DMAN has been studied in aqueous solution. To fully analyze the photophysical behavior of DMAN organic dye, six solutions were prepared in aqueous media at different pHs and concentrations: acidic (pH = 2), neutral (pH = 7), and basic solutions (pH = 12), at two concentrations, diluted ($7\cdot 10^{-5}$ M) and concentrated ($7\cdot 10^{-3}$ M). The photophysics of DMAN in the protonated state (pH < pk_a) is shown in Table S3 and Figure S4. Both diluted and concentrated DMAN-H^+ species at acidic (pH = 2) and neutral (pH = 7) conditions present similar characteristics, with the main absorption band at 285 nm and an emission peak at around 462

nm, in agreement with published data.[1] The very large Stokes shift ($\Delta\upsilon_{St}$ ≈ 13500 cm^{-1}, Table S3) observed for the monoprotonated species is a consequence of the formation of a strongly relaxed and highly polar intramolecular Charge Transfer process (intraCT), involving motions of the DMA groups (dimethylamines) in the excited state.[1–3] The electrostatic potential map of DMAN in Figure S4b suggests a strong charge-transfer character of the molecule with a highly partitioned electronic distribution between the DMAs and the naphthalene moiety. The ICT shows weak emissive capability, resulting in a fluorescence quantum yield of around ⩽1%.[1]

Results clearly indicate that self-interactions of DMAN protonated species do not occur in either dilute or concentrated solutions in the studied range (nearly 10^{-2} M). However, a completely different scenario is found in basic media, at pH = 12, approaching the pK_a of the molecule (Figure S4c and Table S3). The main absorption band is located in this case at 345 nm in diluted medium, red-shifted with respect to acid or neutral pH solutions. This displacement to longer wavelengths upon basifying the medium indicates the formation of neutral DMAN.[1] This neutral species, even at diluted solutions, appears to form aggregates, characterized by a long tail up to 700 nm in the absorption spectra (highlighted with purple color in Figure S4c).

Table S3. Photophysical data - absorption (λ_{ab}s) and fluorescence (λ_{fl}) wavelength maxima and Stokes shift ($\Delta\upsilon_{St}$) - of DMAN (aq) at different pHs and concentrations (diluted = $7\cdot10^{-5}$ M and concentrated = $7\cdot10^{-3}$ M).

[DMAN]	pH	λ_{abs} (nm)	λ_{fl} (nm)	$\Delta\upsilon_{St}$ (cm^{-1})
Dil.	2	285.0	475.5	14233
Conc.	2	284.5	462.0	13504
Dil.	7	285.0	462.0	13443
Conc.	7	284.5	462.0	13504
Dil.	12	345.5	448.0	6622
Conc.	12	381.5	442.0	3588

As the concentration increases, the absorption shifts more bathochromically (from 345.5 to 381.5 nm, Table S3) assigned to stronger interactions between DMAN molecules, likely resulting in the formation of J-aggregates in solution. It should be noted that aggregation is visible even to the naked eye showing a solution color switching from transparent to purplish as the concentration increases at this pH (Figure S4d).

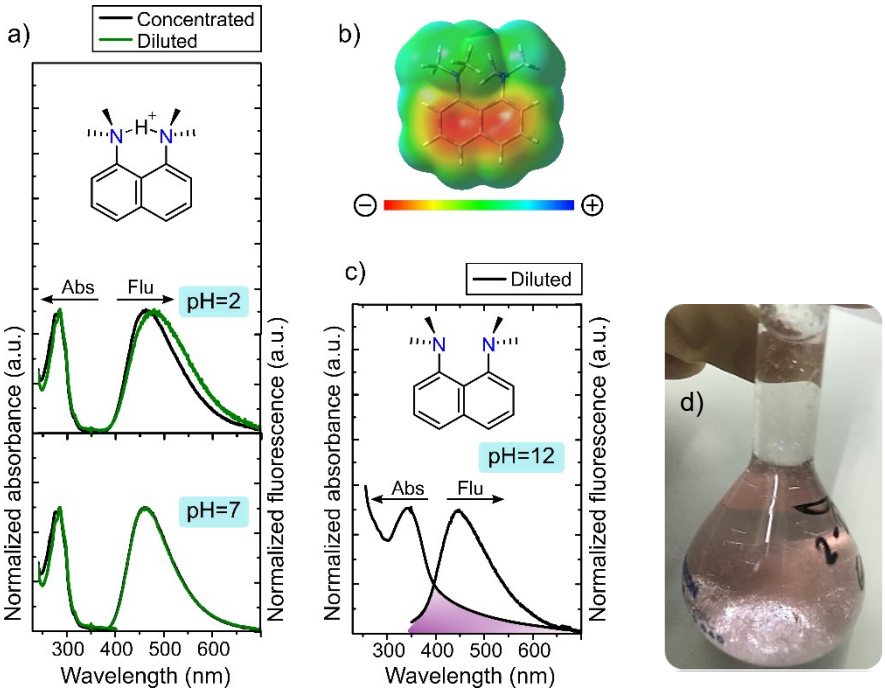

Figure S5. (a) Height normalized absorption and fluorescence spectra of DMAN at different concentrations (diluted = $7{\cdot}10^{-5}$ M and concentrated = $7{\cdot}10^{-3}$ M, green and black lines, respectively) and different pHs. The molecular structure of the protonated species is included. **(b)** Molecular electrostatic potential (MEP) map of DMAN. **(c)** Height normalized absorption, and fluorescence spectra of the diluted DMAN (aq) ($7{\cdot}10^{-5}$ M) at pH = 12. The molecular structure of the neutral species is shown above and the purple filling indicates the formation of aggregates**.** **(d)** Picture of purple solution of the DMAN at concentrated aqueous solution.

Upon excitation to the neutral DMAN (λ_{exc} = 350 nm), the fluorescence spectrum shows its maximum at 445 nm regardless of the solution concentration,[4] which resembles that of DMAN-H^+ in water, but slightly blue shifted (Table S3). This evidence suggests that this emission is still coming from an intraCT state.[3,5]

The differences between the emission of DMAN-H^+ in acid with respect to basic media (DMAN) is related to the more polar character of the CT state in acid pH and a better solvation by water molecules which stabilize it and lead it to lower energies. Another possible explanation may be that DMAN is subjected to important geometrical changes in the excited state, which implies a geometrical relaxation and a reorientation of the dimethylamino groups.[3]

Figure S5 displays the emission of a concentrated sample of DMAN at pH = 12, recorded at high pumping conditions (80 mW power) and at different delay times after the laser pulse upon excitation at λ_{exc} = 460 nm (tail of the absorption spectra). For short delay times, a band centered at 515 nm together with a shoulder at around 600 nm is observed. As the delay increases, the band at shorter wavelengths gradually decreases, and the shoulder at higher wavelengths becomes the main emissive band (delays $\geqslant$ 20 ns). These two bands may imply the formation of two types of aggregates with different relative geometric dispositions in the ground and/or excited state, i.e. the intermolecular charge transfer complex responsible for the red-tail in absorption and the excimers that are only formed in the excited state. Both species are characterized by long lifetimes.[1] Among them, the fluorescence characterized by longer lifetimes (and emission wavelengths) could be related to complexes of intermolecular charge transfer character, while the species with shorter lifetimes (and emission wavelengths) could be assigned to a π-π stacking of the monomers generating excimers in the excited state.[6] The presence of these species completely quenches the emission of monomeric DMAN resulting in quantum yields close to zero regardless of the concentration.[1,3]

In summary, the photophysics of DMAN, the OSDA used for the formation of the ITQ-51 structure, is quite complex, being highly dependent on the pH of the medium and consequently

on the species generated in each state, having a high tendency to self-associate through two types of aggregates in its neutral state.

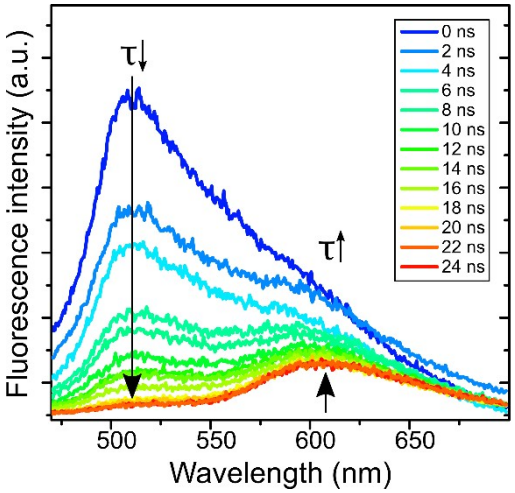

Figure S6. Fluorescence emission spectra for DMAN (aq, pH = 12) at different delay times after laser pulse (from 0 to 24 ns, every 2 ns) upon excitation at 460 nm at a laser power of 80 mW.

References

1 A. Szemik-Hojniak, W. Rettig and I. Deperasińska, The forbidden emission of protonated proton sponge, *Chem. Phys. Lett.*, 2001, **343**, 404–412.

2 R. Martínez-Franco, J. Sun, G. Sastre, Y. Yun, X. Zou, M. Moliner and A. Corma, Supra-molecular assembly of aromatic proton sponges to direct the crystallization of extra-large-pore zeotypes, *Proc. R. Soc. A Math. Phys. Eng. Sci.*, , DOI:10.1098/rspa.2014.0107.

3 A. Szemik-Hojniak, G. Balkowski, G. W. H. Wurpel, J. Herbich, J. H. Van Der Waals and W. J. Buma, Photophysics of 1,8-Bis(dimethylamino)naphthalene in Solution: Internal charge transfer with a twist, *J. Phys. Chem. A*, 2004, **108**, 10623–10631.

4 A. Corma, F. Rey, J. Rius, M. J. Sabater and S. Valencia, Supramolecular self-assembled molecules as organic directing agent for synthesis of zeolites, *Nature*, 2004, **431**, 287–290.

5 R. Martínez-Franco, M. Moliner, Y. Yun, J. Sun, W. Wan, X. Zou and A. Corma, Synthesis of an extra-large molecular sieve using proton sponges as organic structure-directing agents, *Proc. Natl. Acad. Sci.*, 2013, **110**, 3749–3754.

6 V. Martínez-Martínez, S. Furukawa, Y. Takashima, I. López Arbeloa and S. Kitagawa, Charge Transfer and Exciplex Emissions from a Naphthalenediimide-
Entangled Coordination Framework Accommodating Various Aromatic Guests, *J. Phys. Chem. C,* 2012, **116**, 26084−26090.